Journal of Controlled Release 145 (2010) 247–256

Contents lists available at ScienceDirect

Journal of Controlled Release

journal homepage: www.elsevier.com/locate/jconrel

A new approach combining different MRI methods to provide detailed view on swelling dynamics of xanthan tablets influencing drug release at different pH and ionic strength

Urša Mikac [a], Ana Sepe [a], Julijana Kristl [b], Saša Baumgartner [b,*]

[a] Jožef Stefan Institute, Jamova 39, 1000 Ljubljana, Slovenia
[b] Faculty of Pharmacy, University of Ljubljana, Aškerčeva 7, 1000 Ljubljana, Slovenia

ARTICLE INFO

Article history:
Received 15 January 2010
Accepted 18 April 2010
Available online 24 April 2010

Keywords:
Magnetic resonance imaging
Matrix tablets
Nuclear magnetic resonance
Swelling
Xanthan
Drug release
Bio-responsive polymer

ABSTRACT

The key element in drug release from hydrophilic matrix tablets is the gel layer that regulates the penetration of water and controls drug dissolution and diffusion. We have selected magnetic resonance imaging (MRI) as the method of choice for visualizing the dynamic processes occurring during the swelling of xanthan tablets in a variety of media. The aims were (i) to develop a new method using MRI for accurate determination of penetration, swelling and erosion fronts, (ii) to investigate the effects of pH and ionic strength on swelling, and (iii) to study the influence of structural changes in xanthan gel on drug release. Two dimensional (2D) MRI and one dimensional single point imaging (SPI) of swollen xanthan tablets were recorded, together with T_2 mapping. The border between dry and hydrated glassy xanthan—the penetration front—was determined from 1D SPI signal intensity profiles. The erosion front was obtained from signal intensity profiles of 2D MR images. The swelling front, where xanthan is transformed from a glassy to a rubbery state (gel formation), was determined from T_2 profiles. Further, the new combination of MRI methods for swelling front determination enables to explain the appearance of the unusual "bright front" observed on 2D MR images in tablets swollen in HCl pH 1.2 media, which represents the position of swelling front. All six media studied, differing in pH and ionic strength, penetrate through the whole tablet in 4 h ± 0.3 h, but formation of the gel layer is significantly delayed. Unexpectedly, the position of the swelling front was the same, independently of the different xanthan gel structures formed under different conditions of pH and ionic strength. The position of the erosion front, on the other hand, is strongly dependent on pH and ionic strength, as reflected in different thicknesses of the gel layers. The latter are seen to be the consequence of the different hydrodynamic radii of the xanthan molecules, which affect the drug release kinetics. The slowest release of pentoxifylline was observed in water where the thickest gel was formed, whereas the fastest release was observed in HCl pH 1.2, in which the gel layer was thinnest. Moreover, experiments simulating physiological conditions showed that changes of pH and ionic strength influence the xanthan gel structure relatively quickly, and consequently the drug release kinetics. It is therefore concluded that drug release is greatly influenced by changes in the xanthan molecular conformation, as reflected in changed thickness of the gel layer. A new method utilizing combination of SPI, multi-echo MRI and T_2 mapping eliminates the limitations of standard methods used in previous studies for determining moving fronts and improves current understanding of the dynamic processes involved in polymer swelling.

1. Introduction

The criteria used in the design of a drug delivery system are commonly based on the drug's physicochemical and pharmacokinetic properties. Currently, significant efforts are being devoted to developing delivery systems that are responsive to physiological conditions. Water or body fluids hydrate hydrophilic matrix tablets containing the drug, and a hydrogel coat is formed around the dry tablet core. Drug release is a complex process, greatly influenced by the gel layer structure [1–3] that depends on the release medium, the polymer type, surface characteristics, and thermodynamic parameters [4,5]. The various layers formed within matrix tablets during hydration are important in controlling release of the drug. The central dry core is a glassy state polymer. As the medium penetrates into the tablet, a penetration front between the dry glassy and the hydrated glassy polymer appears. As the proportion of the medium increases, the polymer glass transition temperature is reduced to below the system temperature, and the hydrated glassy polymer is progressively transformed to a rubbery state (gel). The interface between the glassy

* Corresponding author. Tel.: + 386 1 4769 633; fax: + 386 1 42 58 031.
E-mail address: sasa.baumgartner@ffa.uni-lj.si (S. Baumgartner).

0168-3659/$ – see front matter © 2010 Elsevier B.V. All rights reserved.
doi:10.1016/j.jconrel.2010.04.018

and rubbery states is called the swelling front. The polymer chains swell as they hydrate, and the eroding front appears as an interface between the swollen tablet and the bulk medium [6,7]. However, much still remains to be learned about swelling of matrix tablets, which could provide significant benefits for their use.

Hydrophilic, non-ionic polymers of semi-synthetic origin (hydroxypropylmethylcellulose—HPMC, hydroxyethylcellulose—HEC, hydroxypropylcellulose—HPC) are commonly used for controlled release from tablets. Polymers of a natural origin, such as xanthan (XAN), are becoming more and more important in the development of modified-release matrix tablets [8–10]. Xanthan is a well known biopolymer that adopts a double-strand helix conformation in its native state [11]. It is a polysaccharide consisting of a cellulose backbone and trisaccharide side chains containing glucuronic acids and a pyruvate group, and responds to external stimuli by exchanging intra- and inter-molecular interactions, causing a variety of polymer conformations. In solution the rigid helix–coil structure transforms into flexible coils [12] whose stability and physical properties are strongly influenced by pH and the ionic environment [8,10,13]. Since these parameters progressively change in the gastrointestinal tract (GIT) [14], it is important to understand the swelling behavior of xanthan tablets under different conditions of pH and ionic strength.

The polymer swelling process has been studied by a variety of techniques [2,3,15,16]. Imaging methods have been used to examine the gel formation in matrix tablets in dissolution media to determine factors that control drug release. Magnetic resonance imaging (MRI) has been used extensively [4,17–23], in particular to investigate HPMC–water systems under different experimental conditions.

Hydrogel formation and the concentration gradient across the gel layer have been measured on the basis of a phenomenological equation [20]. Further improvements for determining polymer concentration profiles across swollen cellulose ether tablets have been reported, in which models were developed on the basis of water proton NMR relaxation parameters combined with MRI data, revealing the concentrations and mobilities of water and polymer as functions of time and distance [4]. Katzhendler et al. studied the microstructure, mobility, internal pH and state of the water in hydrated HPMC matrices containing naproxen sodium and naproxen, using NMR parameters [24]. NMR properties including spin-density and T_2 relaxation times were used to study the swelling kinetics of HPMC at two different pH values [23]. Some interesting conclusions were drawn by Ferrero et al., who used pulsed field gradient nuclear magnetic resonance (PFG-NMR) for measuring the self-diffusion of sodium salicylate in different cellulose ethers [18]. They showed that solute self-diffusivity in hydrogels is not affected by the nature of the cellulose derivative, but is dictated by the solvent viscosity and by the steric obstruction caused by the polymeric matrix that lengthens the drug diffusional path. In all these studies, the swelling front was determined by the appearance of an MRI signal inside the tablet. Since T_2 of the gels at high polymer concentrations can be too short to give any MR signal, the resulting gel thickness measured by the spin-echo sequence could be underestimated. Additionally, this method does not allow differentiation between hydrated glassy and rubbery polymer state.

There have been numerous detailed studies using MRI to investigate non-ionic synthetic polymers, but none on xanthan as an anionic polymer of natural origin. We have proposed that pH and ionic strength of the medium influence the swelling dynamics and gel formation of xanthan matrix tablets, and consequently have an influence on drug release kinetics. To test this, a new method utilizing combination of SPI, multi-echo MRI and T_2 mapping was developed for accurately determining moving fronts during the swelling of xanthan tablets: the penetration, swelling and erosion front. This method eliminated the limitations of standard MRI methods used in previous studies and improved current understanding of the dynamic processes involved in xanthan swelling. Further, it enabled interpretation of the unusual 2D MR images of xanthan tablets swollen at low pH. Moreover, our experiments demonstrate that changes in pH influence xanthan chain hydration relatively quickly, since xanthan behaves as a bio-responsive polymer that adopts different structures under different micro-environmental conditions.

2. Materials and methods

2.1. Materials

Xanthan with a molecular weight of $2 \cdot 10^6$ was obtained from Sigma-Aldrich Chemie, Germany. Pentoxifylline, a methylxanthine derivative, (MW = 278.31) with a solubility in water at 37 °C of 191 mg/ml was supplied by Krka, d.d., Slovenia. Six different media were used: purified water, HCl at pH 3.0 and HCl at pH 1.2 according to Ph. Eur. 6th Ed. and the same media with increased ionic strength (11.7 g of NaCl per 1000 ml of each medium). The final ionic strengths of the media were: water ($\mu = 0$ M), water + NaCl ($\mu = 0.2$ M), HCl pH 1.2 ($\mu = 0.08$ M), HCl pH 1.2 + NaCl ($\mu = 0.28$ M) and HCl pH 3.0 ($\mu = 0.001$ M), HCl pH 3.0 + NaCl ($\mu = 0.201$ M).

2.2. Preparation of matrix tablets

Xanthan and the drug (pentoxifylline) in a 3:1 ratio were mixed homogeneously using a laboratory model drum blender. Circular flat-faced tablets containing 100 mg drug were prepared by direct compression (SP 300, Kilian & co., Cologne, Germany) to form tablets with mass of 0.40 g ± 0.01 g, diameter of 12 mm and crushing strength of 100 N ± 10 N.

For NMR and MRI experiments tablets without drug were prepared with mass of 0.50 g ± 0.01 g, diameter of 12 mm and thickness of 4.0 mm ± 0.05 mm. Before measurements, the moisture content of tablets was determined to be 7% ± 1%, therefore xanthan concentration at room humidity is $c = 0.93 \pm 0.01$. For MRI experiments tablets were covered with a double layer of an impermeable hydrophobic polymer (nitrocellulose in a form of nail polish) applied in a liquid state, leaving only one circular surface exposed for the medium penetration.

2.3. Preparation of xanthan gels at known concentrations

Gels of mass ratio (w/w) ranging from 0.1 to 0.4 xanthan were prepared with all six media. Precisely weighed xanthan was dispersed in the medium with a magnetic stirrer until a uniform gel was formed.

2.4. NMR relaxation times of xanthan gel and xanthan tablet

The NMR spin–lattice (T_1) and spin–spin (T_2) relaxation times were measured at room temperature at a ^{1}H NMR frequency $\nu_H = 100$ MHz for hydrogels of known xanthan concentration. The experiments were performed on a TecMag Apollo (USA) MRI spectrometer with a superconducting 2.35 T horizontal bore magnet (Oxford Instruments, UK) equipped with gradients and RF coils for MR microscopy (Bruker, Germany). The T_1 time was measured by the standard inversion recovery sequence [25] (180°–τ–90°–AQ) by changing τ values from 0.02 ms to 15 s. T_1 value was determined from measurements by fitting the signal intensity (S) obtained at different τ values to

$$S(\tau) = a_1\left(1 - b_1 \cdot e^{-\tau/T_1}\right) \quad (1)$$

where a_1 and b_1 are constants ($b_1 \approx 2$). The T_2 times of gels were measured using the CPMG pulse sequence [26] (90°–τ–[180°–τ–AQ–τ]$_N$) with $\tau = 1$ ms and $N = 3000$. The T_2 times of tablets at room humidity and of completely dried tablets were measured by a Hahn-

echo pulse sequence by changing the inter-echo time from 0.02 ms to 2 s. The T_2 values were determined from

$$S(\tau) = a_2 + b_2 e^{-\tau/T_2}, \quad (2)$$

where a_2 and b_2 are constants.

2.5. MR imaging of xanthan gels and matrix tablets during swelling

MR images were recorded with the same spectrometer as used for the relaxation time measurements. For 2D MR imaging, gels at known xanthan concentrations were placed in an inner container, which was inserted in a larger outer container filled with the medium used as a reference i.e. phantom. The 2D MR images were taken using a standard multi-echo pulse sequence with an echo time (*TE*) of 6.2 ms, number of echoes (*N*) 50 and a repetition time (*TR*) of 200 ms. The field of view was 50 mm with in-plane resolution of 200 μm and slice thickness of 3 mm.

To follow changes of xanthan tablets during swelling, 2D MRI and one dimensional single point imaging (1D SPI) sequences were used after the medium was added to a tablet inserted in a container. A tablet at room humidity was used as reference. The first MR image was taken approximately 10 min after the tablet came in contact with the medium and then every 30 min for 12 h. Additional images were taken after 24 h and at even longer times for some media. This was repeated at least three times for each medium. To simulate swelling in GIT, experiments were carried out with HCl pH 1.2 + NaCl medium, which was replaced after 2 h by water at pH 5.7.

To measure short T_2 times (tablet at room humidity, hydrated glassy polymer and gels with high polymer concentration), a 1D SPI T_2 mapping sequence was used [27]. A single point on the free induction decay was sampled at the encoding time $t_p = 0.17$ ms after the radiofrequency detection pulse $\alpha = 20°$. *TR* was 200 ms and the inter-echo time was varied from 0.3 ms to 10 ms. The field of view was 45 mm with in-plane resolution of 350 μm.

2D MRI signal intensity profiles were determined from 2D images with $N = 1$ ($TE = 6.2$ ms) and 1D SPI signal intensity profiles from SPI measurements at an inter-echo time of 0.3 ms. T_2 mapping was obtained at different swelling times. T_2 values at each point in the 2D MR image were determined by fitting the signal intensities at different echo times to Eq. (2). In the regions with T_2 values shorter than 5 ms, T_2 was obtained from 1D SPI measurements.

2.6. Drug release from xanthan tablets

Dissolution was measured with a fully calibrated dissolution apparatus, using the paddle method (Apparatus II, VanKel Dissolution Apparatus, model VK 7000, USA). In addition to the standard apparatus II arrangement, further variations were made as described [28]. The paddle speed was 50 rpm, temperature 37 °C ± 0.5 °C and volume of the medium 900 ml. At predetermined time intervals, 10 ml samples were withdrawn without replacement. The collected samples were filtered through the 10 μm filters, suitably diluted with the release medium and the absorbance was measured spectrophotometrically at the 274 nm (HP diode array UV–VIS spectrophotometer, 8453, Germany). Experiments were performed with all six media and under simulated physiological conditions, where drug release was followed for 2 h at pH 1.2 and longer in water at pH 5.7. The released drug amounts were calculated using calibration curves.

2.7. Statistical analysis

The values reported are means and standard deviations of experiments carried out at least three times. Data were analyzed using one-way analysis of variance (*t*-test) and $P < 0.05$ was considered significant.

3. Results

3.1. T_1 and T_2 of gels at various values of pH and ionic strength

The mobility of protons within the gel was determined by measuring the relaxation times T_1 and T_2 of gels at known concentrations. Fig. 1 shows relaxation rates ($1/T_1$ and $1/T_2$) of gels prepared with various media. $1/T_1$ and $1/T_2$ were greater when polymer mass ratio was increased from 0 to 0.4, indicating the presence of considerable interactions between the medium and the xanthan molecules, the most probable binding sites being the hydroxyl and carboxyl groups. Mono-exponential decay was observed for all T_1 and T_2 measurements, indicating fast exchange of water molecules between their bound and free states. Differences in T_1 relaxation rates for gels formed with media at different values of pH and ionic strength were negligible, while T_2 relaxation rates for HCl pH 1.2 gels were significantly higher than for other media (Fig. 1). This can be interpreted in terms of structural ordering of water molecules in the gel networks. The higher spin–spin relaxation rates are the consequence of the shorter T_2 of bound water, which depends on the correlation time due to hindered rotation of bound water as well on the tumbling of polymer molecules to which the water molecules are bound [29]. The higher T_2 relaxation rates in HCl pH 1.2 media can therefore be interpreted in terms of more restricted mobility of xanthan chains in low pH media than in water or pH 3.0. These results are consistent with rheological studies which showed that pH decrease or ionic strength increase leads to a more rigid gel

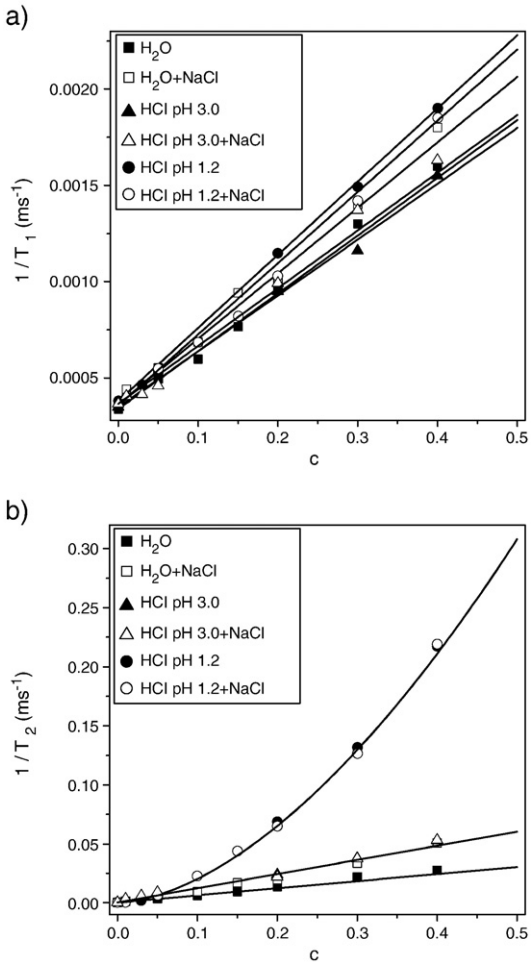

Fig. 1. The relaxation rates (a) $1/T_1$ and (b) $1/T_2$ for gels at different xanthan concentrations *c* (w/w) prepared in six different media: water, water + NaCl, HCl pH 1.2, HCl pH 1.2 + NaCl, HCl pH 3.0 and HCl pH 3.0 + NaCl. The lines are the best fits of the measured data to Eq. (3).

structure [9,30,31]. At low pH or at ionic strengths above 0.15 M the repulsion of ionized xanthan groups is reduced and the polymer assumes a rigid helical rod configuration [10,12]. These differences are less expressed in T_1 relaxation since other modes of relaxation are involved in spin–lattice relaxation.

The influence of low pH or high ionic strength on T_1 and T_2 was described more exactly by fitting $1/T_1$ and $1/T_2$ values to Eq. (3).

$$\frac{1}{T_i} = c^n r_i + \frac{1}{T_{i0}} \tag{3}$$

T_{i0} and T_i are the relaxation times of the medium and the gel, c is the polymer concentration (w/w), r_i is the relaxivity, n the factor of curvature and $i=1$ and 2 for T_1 and T_2 [32]. T_{i0} values are the measured relaxation times of pure medium, while relaxivities r_1 and r_2 and the factor of curvature n result from fitting the measured T_i values at various polymer concentrations to theoretical values from Eq. (3).

The results of fitting obtained for each medium (Table 1) are consistent with the small differences in measured T_1 rates, since r_1 for gels prepared in different media is very similar. On the other hand, the greater differences in T_2 relaxation rates are supported by the greater differences in r_2 values mainly observed at low pH (Table 1, Fig. 1). Increased ionic strength however has a smaller effect on T_2 relaxation rates, leading to smaller differences of r_2 values. The relationships obtained between xanthan gel concentration and $1/T_1$ and $1/T_2$ enable derivation of the theoretical MRI signal intensities.

3.2. MR imaging of xanthan gels and calculation of their signal intensities

The theoretical MR signal intensity of xanthan gels at different concentrations can be obtained [25] from the dependence of the 2D MR signal intensity, S, obtained from T_1 and T_2 values and from selected experimental parameters:

$$S = k\cdot\rho\cdot e^{-(TE/T_2)}\cdot\left(1-e^{-(TR/T_1)}\right), \tag{4}$$

k is a constant independent of the polymer, ρ is proton density, TE is echo time and TR is repetition time. T_1 and T_2 are values for polymer concentration c according to Eq. (3). T_2 of polymer protons is $\approx$0.02 ms, which it is too short to contribute to S, so ρ represents the water proton density proportional to $(1-c)$.

Theoretical normalized signal intensities $S(c)/S(0)$ were calculated for gels with different amounts of polymer at MRI parameters $TE=6.2$ ms and $TR=200$ ms (Fig. 2). $S(0)$ is the signal of the medium. In order to follow hydration characteristics during swelling, imaging parameters were set in such a way that the acquisition times were not too long (i.e. short TR). Echo time (TE) was kept as short as possible but, due to the very short T_2 of the gels at high xanthan concentrations, MR images were both T_1 and T_2 weighted.

The relationship presented in Fig. 2 was first verified for gels at known polymer concentrations from 0 to 0.4 (w/w). Comparison of measured and theoretical values of $S(c)/S(0)$ shows that the relationship between gel concentration and the MR signal intensity calculated from Eqs. (3) and (4) is valid, at least in the concentration range used. $S(c)/S(0)$ for gels prepared in pH 1.2 medium, with or without NaCl, is practically identical (Fig. 2), but differs significantly for gels prepared in other media. Addition of NaCl changes $S(c)/S(0)$ only for gels prepared in pure water. These verified models enable further explanation of 2D MR images of xanthan tablets during swelling.

Table 1
Results of $1/T_1$ and $1/T_2$ curves fitted to Eq. (3). T_{10} and T_{20} are the spin–lattice and spin–spin relaxation times of the medium, respectively; r_1 and r_2 are the relaxivities, n_1 and n_2 are the factors of curvature.

Medium	T_{10} [ms]	r_1 [ms^{-1}]	n_1	T_{20} [ms]	r_2 [s^{-1}]	n_2
H_2O	2950	0.0030	1	2486	0.06	1
H_2O + NaCl	2752	0.0034	1	2424	0.12	1
HCl pH 1.2	2634	0.0039	1	2371	1.00	1.7
HCl pH 1.2 + NaCl	2810	0.0037	1	2810	1.00	1.7
HCl pH 3.0	2872	0.0029	1	2466	0.12	1
HCl pH 3.0 + NaCl	2734	0.0030	1	2548	0.12	1

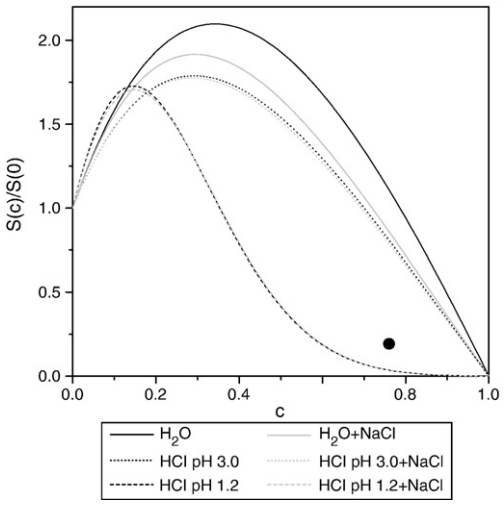

Fig. 2. Normalized MRI signal intensity as a function of xanthan concentration c (w/w), for all six media (lines) and for maximally hydrated glassy xanthan polymer (filled circle) according to Eq. (4). MRI signal intensity S is dependent on the sample characteristics, on T_1 and T_2, and on the experimental parameters TR (repetition time) and TE (echo time) chosen for the spin-echo imaging protocol.

3.3. MR imaging of xanthan tablets during swelling

The signal intensity, seen as brightness on 2D MR images (Fig. 3), results from the chosen experimental conditions and the differences in the physical state of the water during xanthan hydration, expressed by changes in T_1 and T_2. The 'dry' tablet core (the tablet at room humidity, where the polymer concentration (w/w) is $c\approx0.93$) is black in the MR image, since there is only a small amount of water and T_2 is too short to give any 2D MRI signal. The brightness of the newly formed gel is dependent on polymer concentration (Fig. 3a).

After contact of the dry tablet with water the brightness changes along the horizontal direction from black, dry tablet core, through grey gel with high polymer concentration to white, and again to grey (weak signal of free water above the tablet) (Fig. 3b). Despite that at longer times the dry matrix hydrates, the MR signal is low (dark grey), due to high polymer concentration and thus short T_2. On MR images after 13 h of swelling in water, an unexpected black area was observed within the gel layer (black arrow on Fig. 3b). This was attributed to air filling the space arising from the tearing away of part of the gel due to the rapidity of swelling. This area disappeared at later times as air diffused and small air bubbles distributed throughout the whole sample were observed. After 24 h, the whole image in the region of the initial tablet becomes brighter due to high water ingress. Above the white region the signal becomes darker as the amount of polymer decreases. At 66 h the image intensity is uniform inside the whole sample containing homogeneously dispersed small air bubbles. Similar behavior patterns are seen for tablets swelling in water + NaCl, HCl pH 3.0 and HCl pH 3.0 + NaCl (data not presented).

However, in HCl pH 1.2, a significantly different behavior is observed with and without NaCl (Fig. 3b). A bright region is observed next to the

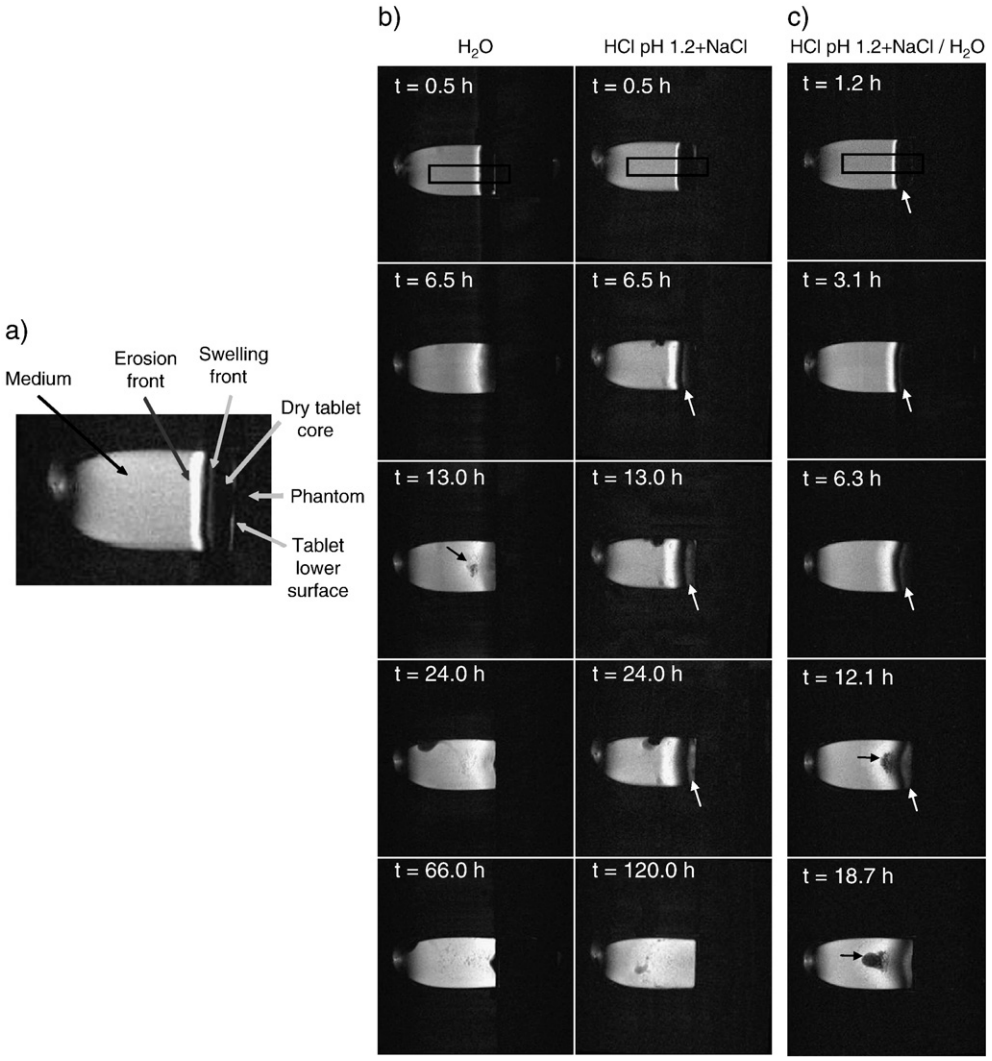

Fig. 3. 2D MR images of xanthan matrix tablets during swelling in different media. (a) The position of the xanthan tablet during the MRI experiment with denoted areas and fronts forming during tablet swelling, as observed on MR images (XAN tablet in HCl pH 1.2 + NaCl medium after 2 h of swelling). (b) A set of MR images of xanthan tablets during swelling in two media at different times. Rectangles on the images at $t = 0.5$ h denote the areas chosen for signal intensity profiles across the swollen tablets. (c) A set of MR images of xanthan tablets during swelling under simulated physiological conditions. HCl pH 1.2 + NaCl medium was replaced by water 2 h after swelling. The signal intensity within the images is displayed using a grey scale where black corresponds to zero signal. Black arrows indicate the positions of empty spaces and white arrows the positions of "bright fronts". The MR images were taken using a standard multi-echo pulse sequence with an echo time of 6.2 ms and a repetition time of 200 ms. The field of view was 50 mm with in-plane resolution of 200 μm and slice thickness of 3 mm.

HCl medium, but an additional one is seen next to the dry tablet core (white arrows on Fig. 3b). This unusual "bright front" appears approximately 30 min after contact of the tablet with the medium and moves inside the tablet with the dynamics of tablet hydration. At 120 h it disappears and the image intensity is uniform throughout the whole sample. These unexpected MR images of tablets swollen in HCl pH 1.2 were further investigated using a combination of 2D MRI and 1D SPI, together with theoretical signal intensity and T_2 mapping across the swollen tablet as is described in Section 3.4.

To simulate the swelling at physiological conditions as the tablet proceeds from stomach to small intestine, xanthan tablet was 2D MR imaged for 2 h in HCl pH 1.2 + NaCl medium and then in water (Fig. 3c). At times shorter than 2 h, swelling was the same as that observed at pH 1.2, later swelling was similar to that in water. However, the "bright front" remained from the HCl pH 1.2 + NaCl medium and it is slowly widened toward the lower edge of the tablet. After approximately 12 h, a dark area (black arrow on Fig. 3c) was attributed to air filling the space arising from tearing away part of the gel due to the fast swelling of xanthan in water.

3.4. Determination of penetration, swelling and erosion fronts

To enable the interpretation of the unusual 2D MR images of xanthan tablets observed at low pH, the current understanding of the dynamic processes involved in xanthan swelling should be improved. Therefore, a new approach was used for determining front positions within the swollen tablet, combining measurements of 1D SPI, 2D MRI and results of T_2 mapping (Fig. 4). Fig. 4 illustrates swollen tablet in water—(a) or in HCl pH 1.2 + NaCl—(b) together with normalized MRI signal intensities and T_2 profiles along the horizontal direction. Furthermore, penetration, swelling and erosion fronts are presented.

From 1D SPI measurements at different swelling times, the penetration front was determined as the position where 1D SPI signal intensity increases above the signal intensity of the tablet used as a reference (Fig. 4, red lines). The border between the bulk medium and polymer, i.e. the erosion front, was obtained from one dimensional signal intensity profiles of 2D MR images in the horizontal direction, at the position where the signal intensity starts to increase above the value of the bulk medium (Fig. 4, black lines).

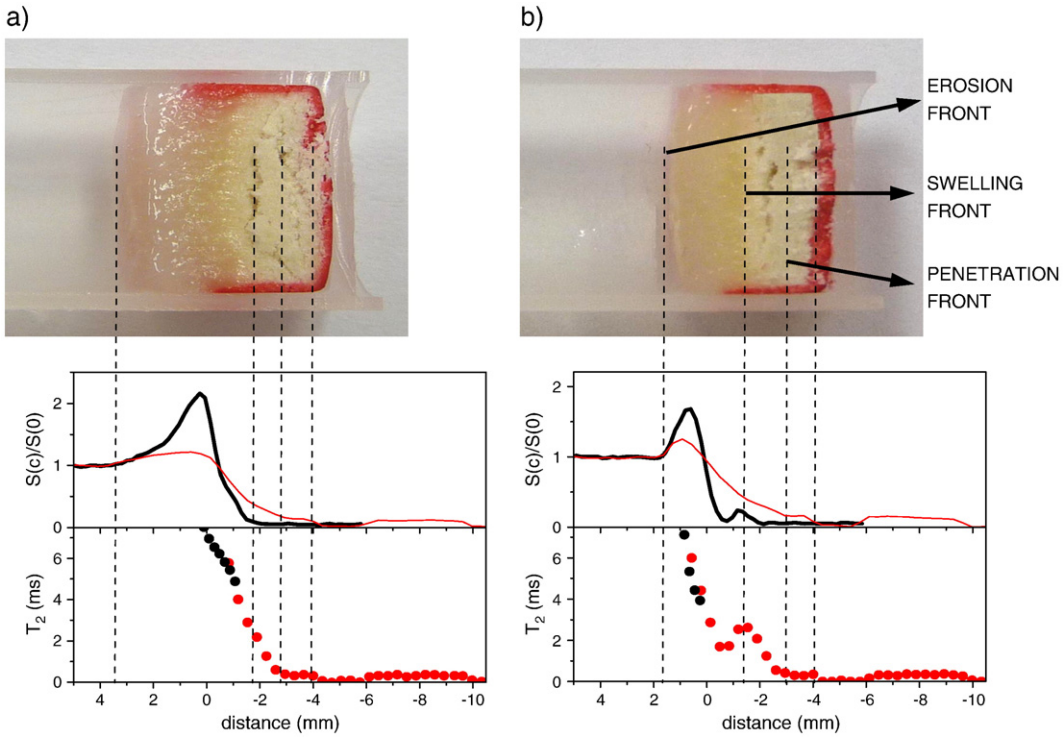

Fig. 4. Photographs of hydrated xanthan tablets after 3 h of swelling in (a) water and (b) HCl pH 1.2 + NaCl, together with 2D MRI (black line) and 1D SPI (red line) normalized signal intensities and T_2 profiles that were obtained just before removing the medium and cutting the tablet along the horizontal direction. T_2 values were determined from 2D T_2 maps for T_2 values longer than 5 ms (●) and from 1D SPI measurements for shorter T_2 values (●). The hydrated glassy polymer is white; the hydrated rubbery polymer is colored from yellow (gel with high polymer concentration) to transparent color of diluted gel. T_2 values of 2.6 ms correspond to the position of the front between the white and yellow regions in the picture for both media, and represent the swelling front position. Zero on x axis represents the surface of the tablet at the beginning of the experiment.

The swelling front, which is the border between the hydrated glassy and the rubbery polymer, was determined from T_2 profiles of swollen tablets. T_2 maps at different swelling times were derived from 2D MRI measurements (Fig. 4 black dots), but for T_2 values shorter than 5 ms, these values were determined from 1D SPI T_2 measurements (Fig. 4, red dots). The T_2 values measured by MR imaging pulse sequence are underestimated due to diffusional loss of the signal during read gradients [25,33,34]. However, the medium diffusion is slow enough to enable determination of real T_2 values in the region close to the swelling front (hydrated glassy polymer and gel at high xanthan concentration).

To be able to determine the position of the swelling front from T_2 profiles, relaxation times of the hydrated glassy xanthan polymer at the swelling front are required. The tablet was therefore cut into two parts after 3 h of hydration and a thin layer of hydrated glassy polymer just below the gel layer excised (Fig. 4). The relaxation times T_1 and T_2 of this part were determined to be 250 ms and 2.7 ms respectively. The position of the swelling front was thus determined from 1D SPI T_2 maps at $T_2 = 2.7$ ms (Fig. 4, red dots). The value was further confirmed from T_2 profiles of xanthan tablets during swelling in pH 1.2 media, where the maximum T_2 inside the tablet is 2.6 ms ± 0.1 ms (Fig. 4b).

The basis for observations of non-continuous changes in the T_2 profile and in the signal intensity at pH 1.2, as reflected in the appearance of the "bright front" on 2D MR images (Figs. 3 and 4), lies in the different spin–spin relaxation times of glassy and rubbery states of xanthan polymer. As the medium penetrates into the tablet it fills the spaces between xanthan particles and can interact only with the polymer chains at the surface, where the hydrated glassy polymer region is formed. The fraction of free water in this region is consequently relatively large, and T_2 can be longer than T_2 of the region where hydrated polymer is in a rubbery state, with high polymer concentration (Fig. 4b). Thus, for certain conditions during swelling, T_2 can be relatively long even at high polymer concentrations.

The position of T_2 maxima in pH 1.2 media (Fig. 4b, red dots) coincides with the appearance of the "bright front" (Fig. 3b). The signal intensity of the maximally hydrated glassy xanthan polymer was determined from its relaxation times to be $S(c)/S(0) = 0.20$ and is seen as a bright front on MR images (Fig. 3b). However, after the polymer is transformed to the rubbery state, the signal intensity decreases significantly, due to decreased T_2 (Fig. 4).

3.5. Responsiveness of xanthan tablets in media with different values of pH and ionic strength

The responsiveness of xanthan tablets to different media was based on precise determination of the position of moving fronts at different swelling times as shown on Fig. 5a. Gel thickness was calculated as the difference between the erosion and swelling fronts. The erosion front expansion was fastest for the xanthan tablet in water. The influence of pH on the gel expansion rate was clearly seen for tablets in HCl pH 1.2, where erosion was considerably slower than in HCl pH 3.0. Increased ionic strength decreased the erosion front expansion in all media. Surprisingly, the positions of the swelling and the penetration fronts did not differ significantly between the six media. Moreover, the hydration time at which the medium penetrates through the whole tablet was also the same, at 4 h ± 0.3 h, for all six media (Fig. 5a). It was concluded therefore, that the gel layer thickness of tablets in different media follows the differences of the eroding front movement: the thickest gel is formed in water and the thinnest in HCl pH 1.2 + NaCl medium (Fig. 5b). The thickness of the xanthan gel layer is thus influenced by low pH and the presence of NaCl, although the effect of the latter is significant only in water or dilute acid medium.

The influence of changing media on formation of xanthan gel layer is observed not only from MR images, but is also reflected in the gel layer thickness (Fig. 6). Under the simulated physiological conditions

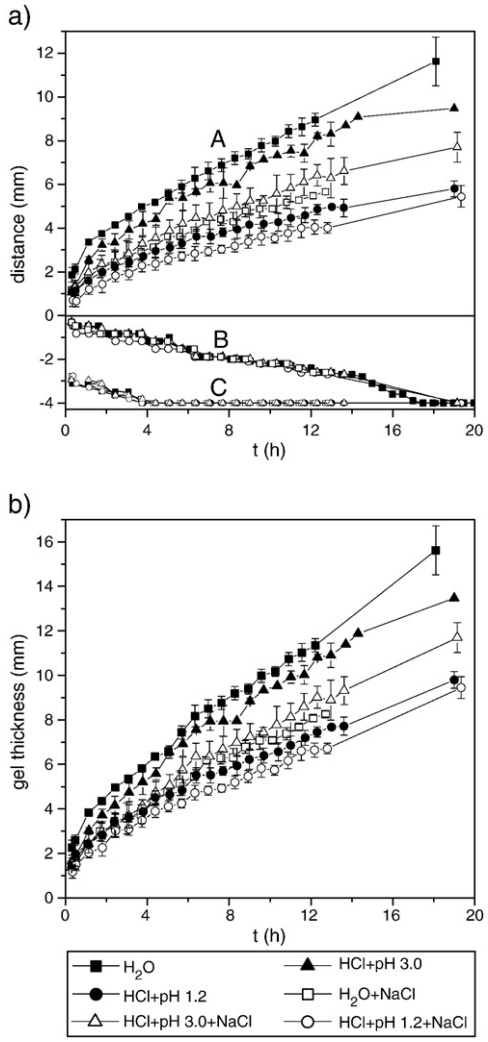

Fig. 5. (a) The positions of erosion (A), swelling (B) and penetration (C) fronts. (b) The increase of gel layer thickness formed in xanthan matrix tablets during swelling in different media. Gel layer thickness is taken as the difference between the erosion and swelling front positions. Each point represents the mean value ± SD.

the gel layer thickness was, for the first 2 h, the same as that in HCl pH 1.2 + NaCl and, after its replacement by water, approached the thickness of the gel in water. It is seen that xanthan matrix tablets respond relatively rapidly to changes in media conditions. Knowledge of the relationship between the characteristics of the medium and the dynamic changes of thickness and structure of the forming gel is important in designing controlled release dosage forms.

3.6. Influence of gel layer on drug release

Pentoxifylline release from xanthan matrix tablets was monitored initially in water, where it was sustained by more than 24 h. In HCl pH 1.2 medium, release of the drug was much faster but, in HCl pH 3.0, only slightly faster than in water (Fig. 7a). Addition of NaCl affects drug release only in water and in dilute acid media (HCl pH 3.0), the effect at pH 1.2 being very small.

The results of drug release performed under simulated physiological conditions, where HCl pH 1.2 medium was followed by water, proved that both the gel layer thickness and also the drug release rate from xanthan tablets respond rapidly to changed environmental conditions (Fig. 7b). The release is much faster during the first 2 h than after the replacement of the medium, indicating that the rates of swelling, and consequently of drug release from xanthan tablets, will differ in the stomach and in the intestine.

4. Discussion

A model describing the swelling, erosion and ultimately gel formation of a hydrophilic matrix was presented by Peppas et al. [35] almost 3 decades ago. In this model, a mechanism for matrix dissolution was described by the movements of the boundaries between the glassy tablet core and the rubbery gel (swelling front) and the gel and the dissolution medium (erosion front). In addition, a front corresponding to the dissolution of the additives in the gel has also been identified (diffusion front). Further, Colombo and colleagues recognize the same three different boundaries [36]. However, an alternative explanation of the fronts, based on previous work of Melia, was provided by Gao and Meury [37], who investigated fronts by optical photography and define additional front named the true penetration boundary, where water has ingressed, but no gel has been formed yet. The penetration front was recognized and proved also by other researchers [18,38], but is still generally misinterpreted and recognized as the swelling front [9,21]. Namely, the position of swelling front is usually determined simply by the appearance of an MRI signal inside the tablet, which depends on the *TE* and *TR* values selected. Different imaging parameters have been used, such as *TE* = 12 ms and *TR* = 1000 ms [21], *TE* = 9.8 ms and *TR* = 300 ms [22] and *TE* = 18 ms and *TR* = 200 ms [4], leading to different positions of the swelling front. Further, for gels at high polymer concentrations, T_2 can be too short, even at the shortest *TE* used, to enable appearance of the MRI signal.

The main disadvantage of 2D MRI technique is that it does not enable imaging of samples with very short T_2 values; therefore, penetration front cannot be accurately determined. During swelling of matrix tablets, T_2 values of the penetration medium as well as T_2 of gel at high polymer concentrations are very short and give no MR signal when spin-echo MRI technique is used. Therefore, the advantage of the SPI technique was introduced, which enables imaging of protons with very short T_2 values and thus makes possible detection of even small amounts of water in a tablet at room moisture. This means that 1D SPI gives density weighted 1D image for medium protons. Therefore, at the position where SPI signal intensity increases above the value of the dry tablet, we were able to determine the position of penetration front accurately.

The results of our experiments demonstrate that the penetration front is not the same as the swelling front since, in the region between these two fronts, xanthan polymer is not in the rubbery state—the

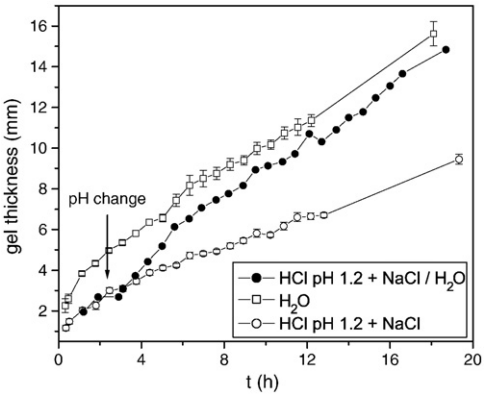

Fig. 6. The gel layer thickness in xanthan matrix tablet during swelling under simulated physiological conditions: HCl pH 1.2 + NaCl medium was replaced after 2 h by water (denoted by arrow). After replacement, xanthan structural changes lead to faster gel expansion, approaching the swelling of xanthan tablets in pure water. For comparison, gel layer thicknesses of xanthan swollen in water and in HCl pH 1.2 + NaCl are presented.

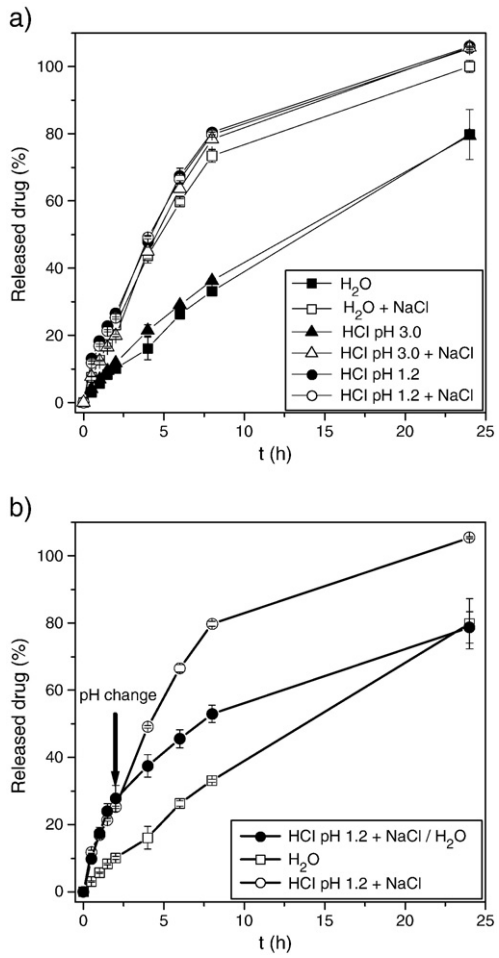

Fig. 7. (a) Release profiles of pentoxifylline from xanthan tablets in investigated media. (b) The influence of medium replacement (denoted by arrow) simulating physiological conditions on the release of pentoxifylline from xanthan tablets: HCl pH 1.2 + NaCl medium was replaced after 2 h by water. For comparison, release of pentoxifylline from xanthan in water and in HCl pH 1.2 + NaCl is presented. Drug release was measured by a modified paddle method (see Materials and methods section) at $T = 37$ °C, $V = 900$ ml, 50 rpm and is presented as mean of 6 measurements. SD is mostly in frame of symbols size.

amount of medium is not sufficient. Only by the combination of 1D SPI, T_2 mapping and 2D MRI results we were able to distinguish rubbery and glassy states of xanthan polymer (Fig. 4), because they differently influence proton mobility. It is reflected in non-continuously changing 2D MRI signal intensities and T_2 profiles of tablets swollen in HCl pH 1.2 media (Fig. 4b, black line and red dots). The position of T_2 maxima coincides with the position of the maxima in signal intensity of 2D MRI, where polymer is in a maximally hydrated glassy state with a significant amount of penetrating medium in pores between xanthan particles. Further interactions of polymer with the medium lead to higher fraction of bound medium and transition of xanthan from glassy to a rubbery state, where T_2 is lower. With ingress of additional amounts of medium, polymer concentration of the formed gel decreases and T_2 increases again to the value of the bulk medium. Similar results on the presence of swelling medium in pores between granules of glassy polymer of the tablet were obtained in studies of gel-forming HPMC tablets combining MRI with scanning microbeam nuclear reaction analysis [39]. It was shown that the medium entered into the tablet faster than gel is formed and faster than observable by the multi-echo MRI technique [19,39,40].

To distinguish T_2 in hydrated glassy and in rubbery state of the polymer T_2 mapping was used. The T_2 of xanthan in a maximally hydrated glassy state being 2.7 ms was determined from a thin layer of the tablet just below the rubbery layer (Fig. 4b). By known T_2 of maximally hydrated glassy polymer, the penetration and swelling fronts can be distinguish combining T_2 profile with 1D SPI signal intensity. The swelling front was thus determined from 1D SPI T_2 maps at $T_2 = 2.7$ ms for all six media. The developed method for determining the swelling front is thus independent of the MRI parameters.

Additional confirmation, that swelling front position was determined correctly is based on 2D MR signal intensity profiles and MR images of xanthan tablets at HCl pH 1.2. As mentioned before, xanthan in glassy and further in rubbery state causes non-continuously changing 2D MRI signal intensities and T_2 profiles as well as the appearance of the "bright front" on 2D MR images. Namely, after the polymer is transformed to the rubbery state, the signal intensity decreases, due to decreased T_2. The T_2 values are at the minimum value of 1.6 ms in HCl pH 1.2 (Fig. 4b), which corresponds to a polymer concentration of 0.76 (Eq. (3)). This concentration is in good agreement with the findings of Shade and Levin, who found that the glass transition temperature T_g of high molecular weight biopolymers is reduced from 200 ± 50 °C (T_g of xanthan is 212 °C [41]) to room temperature if the concentration of water is 0.20 ± 0.05, i.e. at a polymer concentration $c = 0.8 \pm 0.05$ [42]. It is important to stress that the normalized signal intensity $S(c)/S(0)$ at $c = 0.76$ in HCl is only 0.02 (Fig. 2) and MR signal is low. However, for the other four media $S(c)/S(0)$ at this concentration are greater than 0.20 (Fig. 2), and T_2 together with 2D MRI signal intensities change continuously (Fig. 4a). Therefore, no "bright front" is observed for the other four media (Fig. 3).

All the media examined penetrate the tablets at the same rate and, in 4 h were detected in the whole tablet (Fig. 5a). However, the rate of gel formation does not follow penetration rate and the swelling front reaches the lower edge of the tablet after 17 h. Surprisingly, the rate of gel formation is the same for all six media, regardless of the different gel structure.

The erosion and swelling fronts were used to observe the different responses of xanthan swelling under different conditions of pH and ionic strength. The thinnest gel and fastest drug release were observed in HCl pH 1.2 medium (Figs. 5b and 7a). At pH 3.0, the formed gel is thicker and, at pH 5.7 (water medium), the gel is thickest. This pH dependence is expected because of the polyelectrolyte nature of xanthan. It is an acidic polymer with a pKa of 3.1, and is therefore less soluble at pH 1.2 [43] where its carboxylic groups are un-ionized [10,12]. Its interaction with water is thus reduced, affecting gel formation. Swelling is therefore low and drug diffusion through the thin gel layer is fast (Figs. 5b and 7a). At higher pH, ionization of acid groups is enhanced, and solubility and electrostatic repulsion between xanthan chains thus increased. Xanthan polymer is present in a flexible coil conformation in which water is bound to the exposed hydrophilic groups. The latter interactions lead to a thicker gel (Fig. 5b) and slower drug release (Fig. 7a) in water and at pH 3.0.

The presence of NaCl in water or pH 3.0 medium leads to formation of thinner gels and faster drug release (Figs. 5b and 7a), arising mainly from the screening of repulsion between charges on the polymer backbone [44]. The xanthan conformation is changed to rod-like, accompanied by reduction of the hydrodynamic radius [10,45]. The presence of NaCl in pH 1.2 medium has, as expected, a very small effect.

Swelling and drug release studies under simulated physiological conditions showed that soon after replacement of the medium, xanthan conformational changes led to increased hydrodynamic radius, observed as formation of a thicker gel that slowed drug release (Figs. 6 and 7b). Such changes at the molecular level can thus have a rapid impact on macro scale effects, which can sometimes be disadvantageous for drug release *in vivo*, especially in cases where environmentally independent drug release is desired. However, this could be advantageous in case of drugs, where high dosage is required at the beginning and at later times drug concentration is maintained by slower drug release. Swelling of cellulose ethers is less affected by pH and ionic strength [13], therefore matrix effects on drug release in GIT are less expressed.

There have been a lot of studies dealing with hydration properties of non-ionic semi-synthetic polymers like cellulose ethers and its influence of on drug release [4–7,13,46]. Comparison between xanthan and non-ionic polymers reveals that the thickest gel layer in water medium is formed by xanthan, followed by HEC, HPMC and HPC polymers [4,46]. The gel thickness of xanthan strongly depends on medium pH and ionic strength and the gel formed in HCl pH 1.2 + NaCl is even thinner than that of HEC swollen in water. The medium penetration in xanthan is faster compared to penetration of water in tablets of semi-synthetic polymers [46], but the drug release from xanthan tablets in water is slower and of 0 order kinetics. By increasing ionic strength or decreasing pH of the medium, release from xanthan becomes time dependent and comparable with the release rate from HEC polymer tablets [2,13].

At first glance it appears that only gel layer thickness regulates drug release. It is shown here that differences in gel layer thickness are the consequence of different polymer conformations with different hydrodynamic radii. This could explain the contrasting situation in the case of cellulose ethers, where a thinner gel layer leads to slower drug release [5]. To make more quantitative comparison of gel formation events of xanthan tablets versus cellulose ethers and evaluate more precisely different influences on drug release kinetics, further studies by using our new MRI approach are needed. By the knowledge of dynamic processes occurring during swelling of various polymers and their conformations within gel, specific characteristics of each polymer can be exploit for more successful matrix tablets design.

5. Conclusions

A developed new method combining 1D SPI, 2D multi-echo MRI and T_2 mapping enables experimental parameters' independent determination of penetration, swelling and erosion fronts for different types of hydrophilic polymers. In comparison to previously published MRI studies, where swelling and penetration fronts were not possible to distinguish, we were able to accurately determine moving front positions and consequently the gel thickness was obtained with higher precision. The penetration front was determined from 1D SPI profiles, the swelling front from the T_2 value of the maximally hydrated glassy polymer, and the erosion front from signal intensity profiles of 2D MRI. Xanthan hydration depends on pH and ionic strength. Low pH and increased ionic strength were shown to influence xanthan molecular conformation, which constitutes the basis of xanthan bio-responsiveness and adoption of different structures under different micro-environmental conditions. However, these conformational differences are not reflected in the rate of gel formation, i.e. the swelling front position, which was the same for all six media. Xanthan bio-responsiveness was expressed under simulated physiological conditions, in which changes in medium conditions cause alterations at the molecular level, leading to relatively fast changes observed as macro scale effects. It is concluded that drug release is regulated mainly by the structure of the xanthan gel, causing different thickness of the gel layer.

Acknowledgements

This work was supported by the Ministry of Higher Education, Science, and Technology of the Republic of Slovenia. The authors thank Prof. Roger H. Pain for critical reading of the manuscript. Many thanks to Helen Flajšman for valuable technical assistance.

References

[1] C.D. Melia, Hydrophilic matrix sustained release systems based on polysaccharide carriers, Crit. Rev. Ther. Drug Carrier Syst. 8 (1991) 395–412.
[2] S. Baumgartner, J. Kristl, N.A. Peppas, Network structure of cellulose ethers used in pharmaceutical applications during swelling and at equilibrium, Pharm. Res. 8 (2002) 1084–1090.
[3] M. Rahmouni, V. Lenaerts, J.C. Leroux, Drug permeation through a swollen cross-linked amylose starch membrane, STP Pharm. Sci. 13 (2003) 341–348.
[4] S. Baumgartner, G. Lahajnar, A. Sepe, J. Kristl, Quantitative evaluation of polymer concentration profile during swelling of hydrophilic matrix tablets using ^{1}H NMR and MRI methods, Eur. J. Pharm. Biopharm. 59 (2005) 299–306.
[5] S. Baumgartner, O. Planinšek, S. Srčič, J. Kristl, Analysis of surface properties of cellulose ethers and drug release from their matrix tablets, Eur. J. Pharm. Sci. 27 (2006) 375–383.
[6] C. Ferrero Rodrigues, N. Bruneau, J. Barra, D. Alfonso, E. Doelker, Hydrophilic Cellulose Derivatives as Drug Delivery Carriers: The Influence of Substitution Type on the Properties of Compressed Matrix Tablets, in: D.L. Wise (Ed.), Handbook of Pharmaceutical Controlled Release Technology, Marcel Dekker, NY, 2000, pp. 1–30.
[7] P. Colombo, P. Santi, R. Bettini, S.-B. Brazel, N.-A. Peppas, Drug Release from Swelling Controlled Systems, in: D.-L. Wise (Ed.), Handbook of Pharmaceutical Controlled Release Technology, Marcel Dekker, NY, 2000, pp. 183–209.
[8] T. Coviello, F. Alhaique, A. Dorigo, P. Matricardi, M. Grassi, Two galactomannans and scleroglucan as matrices for drug delivery: preparation and release studies, Eur. J. Pharm. Biopharm. 66 (2007) 200–209.
[9] S. Baumgartner, M. Pavli, J. Kristl, Effect of calcium ions on the gelling and drug release characteristics of xanthan matrix tablets, Eur. J. Pharm. Biopharm. 69 (2008) 698–707.
[10] M. Fukuda, N.A. Peppas, J.W. McGinity, Properties of sustained release hot-melt extruded tablets containing chitosan and xanthan gum, Int. J. Pharm. 310 (2006) 90–100.
[11] I. Capron, G. Brigand, G. Muller, About the native and renatured conformation of xanthan exopolysaccharide, Polymer 38 (1997) 5289–5295.
[12] M. Rinaudo, Relation between the molecular structure of some polysaccharides and original properties in sol and gel states, Food Hydrocoll. 15 (2001) 433–440.
[13] M.M. Talukdar, A. Michoel, P. Rombaut, R. Kinget, Comparative study on xanthan gum and hydroxypropylmethyl cellulose as matrices for controlled-release drug delivery I. Compaction and in vitro drug release behaviour, Int. J. Pharm. 129 (1996) 233–241.
[14] J.B. Dressman, R. Berardi, L. Dermentzoglou, T. Russell, S. Schmaltz, J. Barnett, K. Jarvenpaa, Upper gastrointestinal pH in young, healthy men and women, Pharm. Res. 7 (1990) 756–761.
[15] S. Baumgartner, J. Šmid-Korbar, F. Vrečer, J. Kristl, Physical and technological parameters influencing floating properties of matrix tablets based on cellulose ethers, STP Pharm. Sci. 3 (1998) 182–187.
[16] P. Colombo, R. Bettini, N.A. Peppas, Observation of swelling process and diffusion front position during swelling in hydroxypropyl methylcellulose (HPMC) matrices containing a soluble drug, J. Control. Release 61 (1999) 83–91.
[17] J. Craig Richardson, Richard W. Bowtell, M. Karsten, Colin D. Melia, Pharmaceutical applications of magnetic resonance imaging (MRI), Adv. Drug Del. Rev. 57 (2005) 1191–1209.
[18] C. Ferrero, D. Massuelle, D. Jeannerat, E. Doelker, Towards elucidation of the drug release mechanism from compressed hydrophilic matrixes made of cellulose ethers. I. Pulse-field-gradient spin-echo NMR study of sodium salicylate diffusivity in swollen hydrogels with respect to polymer matrix physical structure, J. Control. Release 128 (2008) 71–79.
[19] P.R. Laity, et al., Magnetic resonance imaging and X-ray microtomography studies of a gel-forming tablet formulation, Eur. J. Pharm. Biopharm. 74 (2010) 109–119.
[20] C.A. Fyfe, A.I. Blazek, Investigation of hydrogel formation from hydroxypropyl-methylcellulose (HPMC) by NMR spectroscopy and NMR imaging techniques, Macromolecules 30 (1997) 6230–6237.
[21] K. P. Nott, Magnetic resonance imaging of tablet dissolution, Eur. J. Pharm. Biopharm. 74 (2010) 78–83.
[22] S. Strübing, H. Metz, K. Mäder, Characterization of poly(vinyl acetate) based floating matrix tablets, J. Control. Release 126 (2008) 149–155.
[23] J. Tritt-Goc, N. Pislewski, Magnetic resonance imaging study of the swollen kinetics of hydroxypropylmethylcellulose (HPMC) in water, J. Control. Release 80 (2002) 79–86.
[24] I. Katzhendler, K. Mäder, F. Friedman, Structure and hydration properties of hydroxypropyl methylcellulose matrices containing naproxen and naproxen sodium, Int. J. Pharm. 200 (2000) 161–179.
[25] P.T. Callaghan, Principles of Nuclear Magnetic Resonance Microscopy, Oxford University Press Inc., New York, 1991.
[26] S. Meiboom, D. Gill, Modified spin-echo method for measuring nuclear relaxation times, Rev. Sci. Instr. 29 (1958) 688–691.
[27] S.D. Beyea, B.J. Balcom, P.J. Prado, A.R. Cross, C.B. Kennedy, R.L. Armstrong, T.W. Bremner, Relaxation time mapping of short T_2^* nuclei with single-point imaging (SPI) methods, J. Magn. Reson. 135 (1998) 156–164.
[28] T. Dürig, R. Fassihi, Evaluation of floating and sticking extended release delivery systems: an unconventional dissolution test, J. Control. Release 67 (2000) 37–44.
[29] A. Blinc, G. Lahajnar, R. Blinc, A. Zidanšek, A. Sepe, Proton NMR study of the state of water in fibrin gels, plasma, and blood clots, Magn. Reson. Med. 14 (1990) 105–122.
[30] K.S. Sorbie, Y. Huang, The effect of pH on the flow behavior of xanthan solution through porous media, J Colloid Interface Sci 149 (1992) 303–313.
[31] H. Flajšman, The investigation of swelling of xanthan tablets with oscillatory rheometry and magnetic resonance imaging, Diploma thesis, University of Ljubljana, Slovenia (2008).
[32] V. Mani, K.C. Briley-Saebo, V.V. Itskovich, D.D. Samber, Z.A. Fayad, GRadient echo Acquisition for Superparamagnetic particles with positive contrast (GRASP): Sequence characterization in membrane and glass superparamagnetic iron oxide phantoms at 1.5 T and 3 T, Magn. Reson. Med. 55 (2006) 126–135.

[33] P. Mansfield, P.K. Grannel, Diffraction and microscopy in solids and liquids by NMR, Phys. Rev. B 12 (1975) 3618–3634.
[34] M. Brandl, A. Haase, Molecular-diffusion in NMR microscopy, J. Magn. Reson. B 103 (1994) 162–167.
[35] N.A. Peppas, R. Gurny, E. Doelker, P. Buri, Modelling of drug diffusion through swellable polymeric systems, J. Membr. Sci 7 (1980) 241–253.
[36] R. Bettini, P.L. Catellani, P. Santi, G. Massimo, P.N. Peppas, P. Colombo, Translocation of drug particles in HPMC matrix gel layer: effect of drug solubility and influence on release rate, J. Control. Release 70 (2001) 383–391.
[37] P. Gao, R.H. Meury, Swelling of hydroxypropyl methylcellulose matrix tablets. 1. Characterization of swelling using a novel optical imaging method, J. Pharm. Sci. 85 (1996) 725–731.
[38] G.S. Kazarian, J. van der Weerd, Simultaneous FTIR spectroscopic imaging and visible photography to monitor tablet dissolution and drug release, Pharm. Res. 25 (2008) 853–860.
[39] P.R. Laity, R.E. Cameron, Synchrotron X-ray microtomographic study of tablet swelling, Eur. J. Pharm. Biopharm 75 (2010) 263–276.
[40] G.E. Milroy, R.W. Smith, R. Hollands, A.S. Clough, M.D. Mantle, L.F. Gladden, H. Huatan, R.E. Cameron, The degradation of polyglycolide in water and deuterium oxide. Part II: nuclear reaction analysis and magnetic resonance imaging of water distribution, Polymer 44 (2003) 1425–1435.
[41] R. Khachatoorian, I.G. Petrisor, T.F. Yen, Prediction of plugging effect of biopolymers using their glass transition temperatures, J. Pet. Sci. Eng. 41 (2004) 243–251.
[42] L. Slade, H. Levine, Water and the glass transition-dependence of the glass transition on composition and chemical structure: special implications for flour functionality in cookie baking, J. Food Eng. 24 (1995) 431–509.
[43] M.M. Talukdar, R. Kinget, Swelling and drug release behaviour of xanthan gum matrix tablets, Int. J. Pharm. 120 (1995) 63–72.
[44] H. Frusawa, K. Ito, Polyelectrolyte Properties of Solution and Gels, in: N. Yui, R.J. Mrsny, K. Park (Eds.), Reflexive Polymers and Hydrogels: Underatnding and Designing Fast Responsive Polymeric Systems, CRC Press, London, 2004, pp. 115–143.
[45] D. Bergmann, G. Furth, C. Mayer, Binding of bivalent cations by xanthan in aqueous solution, Int. J. Biol. Macromol. 43 (2008) 245–251.
[46] C. Ferrero, D. Massuelle, E. Doelker, Towards elucidation of the drug release mechanism from compressed hydrophilic matrixes made of cellulose ethers. II. Evaluation of a possible swelling-controlled drug release mechanism using dimensionless analysis, J. Control. Release 141 (2010) 223–233.